Food Chemistry: X 22 (2024) 101459

Contents lists available at ScienceDirect

Food Chemistry: X

journal homepage: www.sciencedirect.com/journal/food-chemistry-x

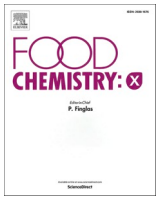

Non-covalent interactions between rice protein and three polyphenols and potential application in emulsions

Xin Huang, Boxue Xia, Yaxuan Liu, Cuina Wang *

Department of Food Science, College of Food Science and Engineering, Jilin University, Changchun 130062, China

ARTICLE INFO

Keywords:
Rice protein
Structure
Functionality
Emulsion

ABSTRACT

Rice protein (RP) and polyphenols are often used in functional foods. This study investigated the non-covalent interactions between RP and three polyphenols (curcumin, CUR; quercetin, QUE; resveratrol, RES) and used the complexes as emulsifiers to create emulsions. Three polyphenols interacted with RP to varying extents, with QUE showing the greatest binding affinity and inducing the greatest alterations in its secondary structure. Molecular docking analysis elucidated the driving forces between them including hydrophobic interactions, hydrogen bonding, and van der Waals forces. Combination with QUE or RES induced structural changes of RP, increasing particle size of complexes. The synergistic effect of polyphenols and protein also enhanced radical scavenging capacity of complexes. Compared to pure protein, all complexes successfully created emulsions with smaller particle size (378–395 nm vs. 470 nm), higher absolute potential (37.43–38.26 mV vs. 35.62 mV), and greater lipid oxidation stability by altering protein conformation.

Introduction

In recent years, novel plant proteins have gained increasing attention as potential substitutes or supplements for animal-based proteins (Ismail, Senaratne-Lenagala, Stube, & Brackenridge, 2020). As an exceptional and cost-effective plant-based protein source, rice protein (RP) has aroused great interest and has been used in various products such as infant formula and beverages (Dai, Chen, et al., 2019). RP possesses remarkable nutritional attributes such as low allergenicity, high digestibility, superior protein efficiency ratio, and well-balanced amino acid profile (Wang, Xu, Chen, Zhou, & Wang, 2018). In addition, RP have many valuable functional properties like emulsifying, foaming, water absorption and oil holding capacity (Roy, Singh, Sari, & Homroy, 2023). Emulsification is currently the most extensively studied property of RP besides solubility. Research has also confirmed that RP is a potential emulsifier to be explored (Sun, Lv, Chen, & Wang, 2019). However, RP contains a large amount of thiol groups and disulfide bonds, leading to poor solubility in water. When only relying on protein stabilization, the performance of the resulting emulsion may be unsatisfactory (Tu, Zhang, & Wang, 2023). Researchers are also investigating different processing methods such as salt treatment, enzymatic hydrolysis, ultrasonic treatment (Ghanghas, Mukilan, Sharma, & Prabhakar, 2022), etc., or combining with other substances such as adding small molecules (Dai, Li, et al., 2019) to regulate the structure of RP and improve its emulsifying properties.

Polyphenols are often used in functional foods as biologically-active phytochemicals from plants (Peng et al., 2019). Covalent binding between protein and polyphenol usually has a better functional effect in stabilizing emulsions. There are also recent studies on the application of covalent interactions between RP and polyphenol (Guo, Wang, Xing, Pan, & Wang, 2023; Pan et al., 2022). In recent years, research on non-covalent interactions between proteins and polyphenols has also been increasing. The interactions can be used to fabricate polyphenol carriers, improving their stability and bioavailability (Chen et al., 2023; Jiang, Gan, Wang, & Lv, 2023). Additionally, the interaction can be applied to alter functional properties of proteins, such as emulsifying and foaming capacity (Han et al., 2022; Pan et al., 2022). Polyphenols interact with protein through various mechanisms such as hydrogen bonding, electrostatic interactions, and hydrophobic interactions, leading to changes in the spatial conformation of protein. Changes in protein structural characteristics, such as surface hydrophobicity, and molecular flexibility, can affect its diffusion rate and adsorption behavior at the oil–water interface of emulsions (Zhang, Fan, Liu, Huang, & Li, 2022), ultimately influencing its emulsification performance (Han et al., 2022). It was also emphasized that the employment of protein–polyphenol complexes as an emulsifier can effectively inhibit lipid oxidation of

* Corresponding author at: Xi'an Road 5333#, Jilin University, 130062, China.
E-mail address: wangcuina@jlu.edu.cn (C. Wang).

https://doi.org/10.1016/j.fochx.2024.101459
Received 30 January 2024; Received in revised form 6 May 2024; Accepted 8 May 2024
Available online 14 May 2024

emulsions during storage (Liu, Gao, Li, & Xie, 2022; Wan, Wang, Wang, Yuan, & Yang, 2014) due to the potent antioxidant ability of polyphenols.

Curcumin (CUR), quercetin (QUE), and resveratrol (RES) are three well-recognized phenolic compounds found in plants. CUR, derived from turmeric rhizome, is a natural phenolic compound (Jiang et al., 2023). QUE, a natural flavonoid found in vegetables, fruits, and medicinal plants (Su, He, & Li, 2022). RES is a polyphenolic substance found in herbs, grapes, apples, and peanuts (Zhong et al., 2023). They all possess significant biological activities such as antioxidant, anti-inflammatory, and anti-tumor properties, and offer various health benefits. Structurally, as shown in Fig. 1, CUR is composed of two *ortho*-methoxy phenols linked by a β-diketone molecule and contains two hydroxyl groups. QUE is a compound composed of two aromatic rings connected by an oxygenated heterocyclic ring and featuring five hydroxyl groups. RES is comprised of two aromatic rings, one double bond, and three hydroxyl groups (Zhou, Zheng, & McClements, 2021). Furthermore, these three hydrophobic polyphenols exhibit differences in molecular weight (CUR > QUE > RES) and lipophilicity order (Log P_{CUR} = 3.2 > Log P_{RES} = 3.1 > Log P_{QUE} = 1.5) (Zhang, Wang, et al., 2022). These structural and property variances may result in differences in their interactions with proteins. Although there have been some reports on the interaction between individual polyphenols and RP, they mainly focus on the aspects of fabrication of carrier and the subsequent protecting effects (Chen et al., 2020; Dai, Li, et al., 2019; Liu et al., 2018; Peng et al., 2017; Xu, Qian, Wang, Chen, & Wang, 2022). Furthermore, research has demonstrated that variations in polyphenol types result in differences in protein–polyphenol interactions (Parolia et al., 2022). However, a comprehensive investigation into the non-covalent binding of the three polyphenols to RP in the aqueous solution and the subsequent applications in emulsions is lacking. Thus, in the present study, the interplay and underlying mechanisms between CUR/QUE/RES and RP were thoroughly explored. Afterwards, the complexes of protein and polyphenol were investigated for the applicability in emulsion. We hypothesize that the structural differences among the three polyphenols may result in variations in their interactions with RP, thus leading to differences in the performance of protein–polyphenol complexes in emulsion applications. Therefore, the objective of this study is to investigate and compare the non-covalent binding mechanisms of the three polyphenols with RP, as well as the effects of the complexes in emulsion applications.

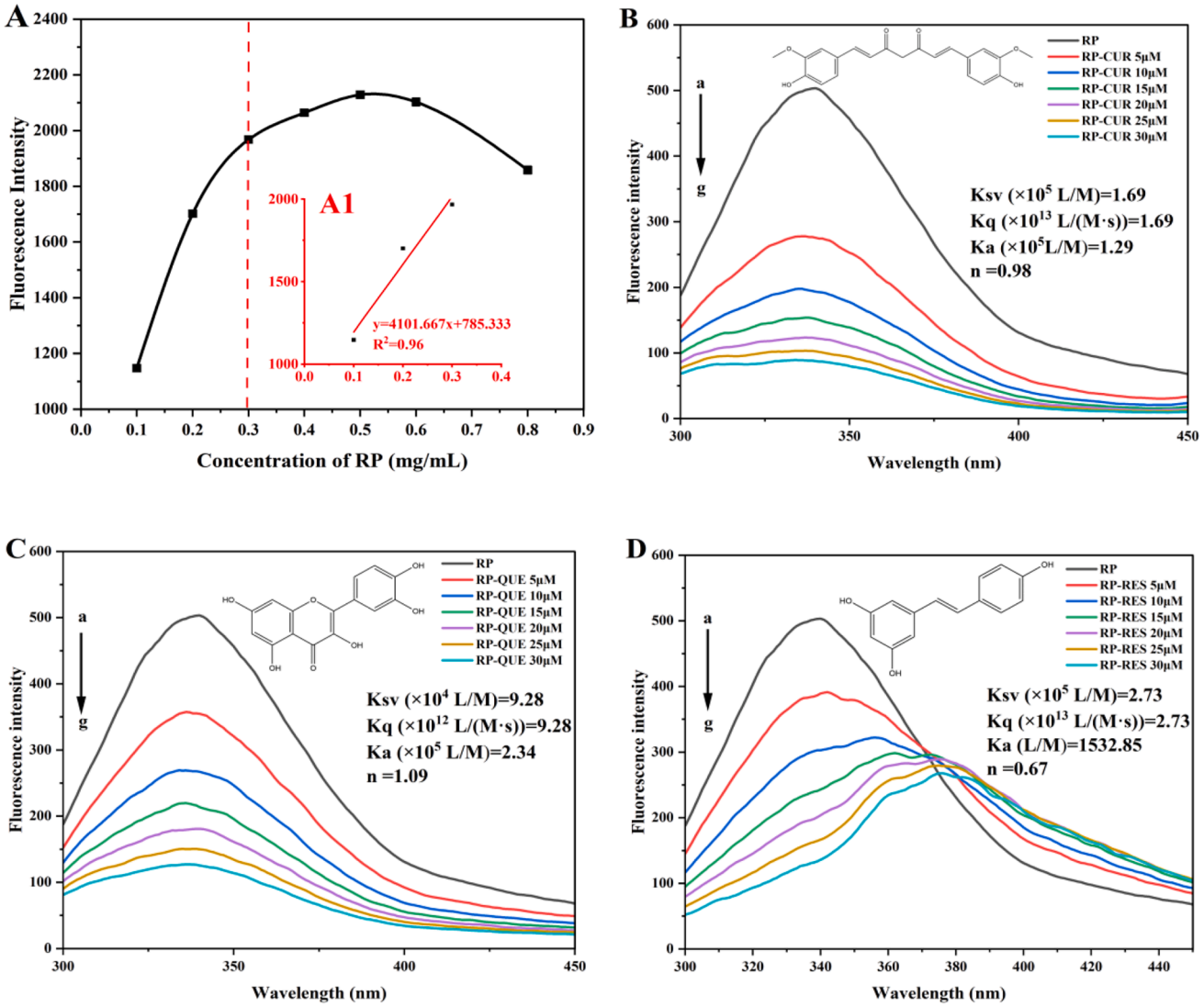

Fig. 1. (A) Fluorescence intensity change with different RP concentrations, and (A1) the plots of three concentrations of RP against the fluorescence intensity. Fluorescence emission spectra of RP in the presence of CUR (B), QUE (C), and RES (D) with concentrations ranging from 0 to 30 μM (a–g). The excitation wavelength was set at 280 nm. Inset: 2D structure of CUR, QUE and RES and calculated parameters using Stern-Volmer and double logarithmic equations.

Materials and methods

Materials

Rice protein (RP, ≥80 %) was donated by Gebiou Technology Co., ltd. (Jiujiang, Jiangxi, China). Quercetin (QUE, ≥97 %, CAS: 117-39-5) and resveratrol (RES, ≥98 %, CAS: 501–36-0) were obtained from Yuanye Bio-tech Co., ltd. (Shanghai, China). Curcumin (CUR, ≥95 %, CAS: 458-37-7) was purchased from Solarbio Life Sciences (Beijing, China). Bicinchoninic acid (BCA) Kit was obtained from Beyotime Biotechnology (Shanghai, China). Potassium bromide (KBr) was provided by Sigma-Aldrich (St. Louis, MO, USA).

Preparation of soluble rice protein solution

A 2 % (w/v) RP suspension was prepared by carefully adding RP powder to ultrapure water, followed by pH adjustment to 12 using a 2 M NaOH solution. The resulting solution was stored at 4 °C for 12 h to ensure proper hydration of the protein (Zhao, Xiong, Chen, Zhu, & Wang, 2020). Once the solution reached room temperature, it was processed using an ultrasonic cell breaker (VCX800, Sonic, USA) with an amplitude of 30 % for a total of 20 min in a cycle of 5 s on and 5 s off. Subsequently, pH of the suspension was adjusted to 7 using a 2 M HCl solution. The suspension was then subjected to centrifugation at 3,000 g for 20 min using a centrifuge (Avanti J-E, Beckman coulter, USA), and the supernatant was collected. The protein concentration was measured using a BCA assay kit.

Preparation of protein–polyphenol complexes

Stock solutions of CUR, QUE or RES were prepared in brown tubes using anhydrous ethanol at a concentration of 10 mM and stored in the dark. Complexes were prepared by adding the polyphenol solution to a RP suspension (0.4 mg/mL) and stirring in the dark for a minimum of 2 h. The final concentrations of polyphenols in the complex solutions were 0–30 μM.

Steady endogenous fluorescence spectroscopy

The steady-state endogenous fluorescence spectra of the RP in the presence of different concentrations of CUR, QUE, or RES were measured using a fluorescence spectrophotometer (Shimadzu, Tokyo, Japan). The emission spectrum was recorded within the range of 300–450 nm, with an excitation wavelength of 280 nm. The fluorescence spectra were acquired at a temperature of 25 °C. The slit widths for both excitation and emission were set at 5 nm. To avoid the influence of polyphenols, the fluorescence background of each individual polyphenol at excitation wavelength of 280 nm was deducted from the spectra of complexes.

UV-absorption spectra measurement

The UV-absorption spectra of the samples were analyzed using a UV-Spectrophotometer (UV-2550, Shimadzu, Kyoto, Japan) within the wavelength range of 240–500 nm. Ultrapure water was used as the control.

Molecular forces

Referring to the method of Li, Wang, Zheng, and Guo (2019) with some modifications, three denaturing agents were employed: NaCl (0.1 M, for disrupting intermolecular forces), SDS (0.1 M, for breaking hydrophobic interactions), and urea (0.1 M, for disrupting hydrogen bonds). The preparation method of the RP-polyphenol complex (polyphenol concentration of 30 μM) is consistent with Section 'Preparation of protein–polyphenol complexes'. The denaturation reagent was added to the sample and stirred for 30 min. The final concentration of urea, SDS, and NaCl in the sample solution was 10 mM. Deionized water was added as a control in the blank group. The fluorescence spectrum was measured using a fluorescence spectrophotometer (Hitachi, Japan) with an excitation wavelength of 280 nm and a scanning range of 300–500 nm.

Computational docking simulation

Computational docking simulation was performed to investigate the mechanism between RP and three polyphenols. Rice glutelin, the predominant protein component in RP, was selected as the model. A reliable homology model of rice glutelin was developed using the structure of pumpkin seed globulin (PDBID: 2EVX_A) sourced from the Protein Data Bank (https://www.rcsb.org/pdb) as a template, which has a sequence identity of about 46 % with rice glutelin (Dai et al., 2017). The three-dimensional structures of CUR (CID: 969516), QUE (CID: 5280343), and RES (CID: 445154) were retrieved from PubChem (https://pubchem.ncbi.nlm.nih.gov/). A docking box with dimensions (60, 60, 60) and grid points spaced 1 Å apart, positioned at coordinates (43.81, 132.401, 38.864) along the xyz axes, was constructed to facilitate the docking simulations. The PyMOL software package was employed for visualizing the binding conformations of the polyphenols with their respective surrounding amino acids at the binding site.

Far-ultraviolet circular dichroism (Far-UV CD) spectra measurement

Samples were diluted with ultrapure water to a protein concentration of 0.2 mg/mL. Far-UV CD spectra were then measured using a CD Spectropolarimeter (MOS-500, Bio-logic, France) with a 1 mm optical path quartz cuvette, covering a spectral range of 190–260 nm. The background signal was obtained using ultrapure water. The quantification of protein secondary structures was conducted using the CONTIN algorithm through the online DichroWeb platform (https://dichroweb.cryst.bbk.ac.uk/).

Fourier transform infrared (FTIR) spectra measurement

The complexes of RP and polyphenol were prepared with the protein aqueous solution concentration of 1 mg/ml and the polyphenol concentration of 75 μM/g protein, and then freeze-dried. The freeze-dried samples (2 mg) were mixed with KBr powder (200 mg) and pressed meticulously to obtain uniform slices. The FTIR spectra of the samples were recorded using an IRPRESTIGE-2 FTIR spectrometer (Shimadzu, Tokyo, Japan) with a resolution of 4 cm^{-1}, spanning the range of 4000–400 cm^{-1}.

Particle size and zeta potential determination

The mean particle size, polydispersity index, and zeta potential were measured using dynamic light scattering at room temperature, employing a Malvern Nano Zetasizer (Malvern Instruments Ltd., United Kingdom). Each sample underwent this measurement procedure at least three times to ensure accuracy and reliability.

Antioxidant properties measurement

The RP samples (0.4 mg/ml) containing varying concentrations of three polyphenols (0–30 μM) were evaluated for their 2,2-diphenyl-1-picrylhydrazyl (DPPH) and 2,2′-azinobis (2-ethylbenzothiazoline-6-sulfonate) (ABTS) free radical scavenging capacity, following the methodology outlined in our previous study (Wang, Cui, Sun, Wang, & Guo, 2022).

Preparation of emulsions

RP supernatant (10 mg/mL) was combined with polyphenols at a concentration of 75 μM/g protein and then thoroughly mixed for at least 2 h in the dark. Subsequently, the complex was mixed with soybean oil at a ratio of 9:1 and immediately subjected to shearing using a high-speed shear (T25, IKA, USA) at 12,000 rpm for 2 min to generate a coarse emulsion. The coarse emulsion was further processed using ultrasound (30 % amplitude, 5 s on, 5 s off) for 5 min to obtain a fine emulsion.

Characterization of emulsion

Particle size and surface charge

The mean droplet size, polydispersity index and zeta potential of emulsions were measured using dynamic light scattering using Malvern Nanosprayer (Malvern Instruments LTD., UK). This measurement procedure is performed at least three times for each sample to ensure accuracy and reliability.

Microstructure observation

Microstructural analysis of the emulsions was conducted using a BX 53 optical microscope (Olympus America Inc.) equipped with a dynamic digital camera at a magnification of 100×. The acquired images were processed and analyzed using MD50-V2 software (Mshot) to extract relevant information.

According to the published method (Cen et al., 2022), the Nile Red and Nile Blue dye solutions were prepared in isopropanol (1 mg/mL), the emulsion samples were diluted 10-fold with deionized water and fully stained by adding 20 μL of Nile Red and 20 μL of Nile Blue dye solution to 1 mL of sample. Laser confocal scanning was performed at excitation wavelengths of 488 nm and 633 nm using a FV 3000 optical microscope (Olympus America Inc., Pennsylvania, USA) equipped with a dynamic digital camera.

Degree of oxidation

The degree of oxidation in the emulsion was evaluated by analyzing the primary and secondary oxidation products formed during storage, as per our previous study (Wang, Zhang, et al., 2022). To this end, the peroxide value (PV) and thiobarbituric acid reactive substances (TBARS) were measured, respectively, during a 10-day accelerated storage test at 55 °C.

Statistical analysis

IBM SPSS Statistics 21 (SPSS Inc. Chicago, IL, USA) was used for statistical analysis of the data, and the results of each group of experiments were the mean of three replicates of at least two batches, and the data were expressed as the mean ± standard deviation. Homogeneity of variance was tested using one-way analysis of variance (ANOVA) and least significant difference (LSD) tests, with $p < 0.05$ considered statistically significant. Plotting was performed using Origin 2023 (OriginLab, Northampton, MA, USA).

Results and discussion

Preparation of soluble rice protein solution

RP is primarily consisting of glutelin, which possesses more than 40 % hydrophobic amino acids, which are easy to aggregation (Xu et al., 2022). Consequently, RP exhibits extremely poor water solubility (less than 2 %) within the pH range of 4–10 (Baek & Mun, 2022; Chen et al., 2022). Thus, improved solubility of RP is crucial for its utilization in the aqueous food systems. To address this issue, we employed processing techniques (extreme alkali treatment and ultrasound) on the RP raw material to enhance its water solubility.

As shown in Fig. S1, the control sample displayed a solubility of approximately 1 % at the neutral pH, which significantly increased to about 28 % after pH-shifting treatment ($p < 0.05$). This improvement can be attributed to the depolymerization of RP aggregates and structural changes induced by the alkali shift treatment (Dai et al., 2022). Combining pH-shifting with ultrasound-assisted treatment further enhanced the solubility of RP. The high shear energy waves and cavitation generated by ultrasound effectively broke down large aggregates into smaller fragments (Liu, Liu, Xiong, Fu, & Chen, 2017). Previous studies have reported the synergistic modification of plant proteins on solubility and emulsification through the combined use of high-intensity ultrasound and pH-shifting technology (Liu et al., 2017). The highest solubility, reaching ~60 %, was achieved after 20 min of ultrasonication. Subsequent decrease in solubility observed at 25 min may be attributed to the agglomeration of the smaller fragments formed by breaking up the larger particles (Zhang et al., 2018). Therefore, the soluble RP solution used in the subsequent experiments was prepared by subjecting the RP suspension to ultrasonication at pH 12 for 20 min, which had a solubility of about 12 mg/mL.

Fluorescence emission spectra

Fluorescence intensity measurements were performed on protein solutions with concentrations ranging from 0.1 to 0.8 mg/mL at an excitation wavelength of 280 nm (Fig. 1A). A linear increase in fluorescence intensity was observed at lower protein concentrations. However, beyond 0.5 mg/mL, fluorescence intensity decreased as protein concentration increased, indicating the presence of self-quenching phenomena (Li, Dai, et al., 2021). Consequently, a protein concentration of 0.4 mg/mL was selected for subsequent fluorescence quenching experiments and analyses.

As shown in Fig. 1B–D, pure RP displayed a fluorescence spectrum with maximum fluorescence intensity wavelength at 343 nm, consistent with a previous study (Dai, Li, et al., 2019; Xu et al., 2019). Upon incorporation of polyphenols, the fluorescence intensity of protein gradually decreased, accompanied by a shift in the maximum wavelength, indicating interactions between the two types of compounds (Lu, Zhao, Wang, Zhang, & Wang, 2022). Results indicated that the fluorophores, mainly tryptophan, was more exposed when the protein was partially or completely unfolded induced by CUR/QUE/RES, causing a decrease in the fluorescence intensity of excited endogenous tryptophan (Huang et al., 2022). Additionally, inclusion of RES led to a pronounced red shift, while QUE and CUR elicited a relatively minor effect towards shorter wavelength direction. This result may be related with the fluorescence properties of CUR, QUE, and RES, which possess the maximal fluorescence wavelength at ~310, ~335, and ~390 nm, respectively.

Fluorescence quenching mechanism

The fluorescence quenching data were analyzed using the Stern-Volmer equation (Equation (1)). Linear plots of fluorescence intensity against polyphenol concentration were observed (Fig. S2), with excellent correlation coefficients ($R^2 > 0.99$), suggesting that the quenching process followed a static mechanism (Dai, Li, et al., 2019). Furthermore, as shown in Fig. 1B–D, the biomolecular quenching rate constant K_q (obtained by multiplying K_{sv} with average lifetime of protein, 10^{-8} s) were calculated to be 9.28×10^{12}–2.73×10^{13} L/M·s, all surpassing the maximum dynamic quenching constant (2.00×10^{10} L/M·s), which support the judgement of static quenching, indicating the formation of complexes between polyphenols and RP at the ground state. Similar findings were reported for rice glutelin and resveratrol (Dai, Li, et al., 2019).

$$\frac{F_0}{F_0 - F} = \frac{1}{f_a} + \frac{1}{f_a \times K_{sv} \times [CUR/QUE/RES]} \quad (1)$$

Where F_0 was the maximum fluorescence intensity of RP, F was the fluorescence intensity of RP quenched by various concentrations of polyphenol. f_a is the accession fraction and K_{sv} is the quenching constant. [CUR/QUE/RES] is the concentration of polyphenols.

For the analysis of the binding constant and number of binding sites in the static quenching process, the following double logarithmic equation (Equation (2)) was employed, the plots are shown in Fig. S2.

$$\log\frac{F_0 - F}{F} = \log K_a + n\log[CUR/QUE/RES] \quad (2)$$

Where K_a is the binding constant and n is the binding number.

Fig. 1 displayed that three polyphenols bound to RP with varied affinity. QUE exhibited the highest binding constant of 2.34×10^5 L/M. RES was calculated to be the lowest with the value of 1.53×10^3 L/M, which was similar with previous study where RES was combined with rice glutelin at a K_a value of 1.44×10^3 L/M (Dai, Li, et al., 2019). The three polyphenols were capable of bind with RP spontaneously and strongly. Previous studies have also reported the strong binding affinities of the three polyphenols to various proteins, such as pea protein (Zhang, Wang, et al., 2022). The number of binding sites for polyphenols in RP was in the sequence of QUE (1.09) > CUR (0.98) > RES (0.67). Apparently, the binding numbers for polyphenols were approximately equal to 1, corresponding to the phenomenon that only one binding location may be present in RP. The binding constants and binding number of the order QUE > CUR > RES may be related to the total number of hydrogen bond donors and acceptors in the three substances (QUE: 12, CUR: 8, RES: 6) as well as their topological polar surface area (QUE: 127, CUR: 90, RES: 67), data from PubChem website.

UV–vis absorption spectra

UV–vis absorption spectrum is a simple and reliable technique to investigate protein conformation alterations. Fig. S3 illustrates the UV–vis absorption spectra of RP mixed with CUR/QUE/RES at various concentrations. The protein exhibited a prominent absorption peak at around 275 nm, attributed to the electronic transitions between π-type molecular orbitals occurs to aromatic rings of aromatic amino acids, as the local environment of tryptophan and tyrosine residues was highly sensitive to this wavelength (Han et al., 2022). As the concentration of CUR/QUE/RES increased, the absorbance of the mixture gradually rose, indicating potential interactions between protein and polyphenols. To ensure the hypothesis, simple sum of absorbance of individual polyphenols at different levels and RP was compared with that of the complexes. And the results demonstrated that they did not overlap, confirming the occurrence of non-covalent interactions between RP and polyphenols (Lu et al., 2022; Zhao et al., 2023). An increase in UV absorption intensity of protein may be due to that hydrogen bonding might occur between polyphenols and protein, because hydrogen bonding increased the intensity of π electron clouds on the aromatic rings of protein and lowered the transition energy, leading to a hyperchromic effect (Ye, Fan, Xu, & Liang, 2013). Furthermore, the intensity of the typical peak was enhanced with increasing polyphenol concentration in a dose dependent manner, confirming the hydrophobic interaction between the aromatic amino acids of protein and aromatic rings from polyphenol (Li, Wang, Zhang, Yu, & Chen, 2021).

Fig. S3 showed that the absorption peak of RP at 275 nm was shifted after the addition of polyphenols. The spectral changes of the peaks can reflect changes in the protein structure and the microenvironment of the protein's aromatic acid residues. The blue-shift of the maximum peak of the complexes after the addition of CUR or QUE, indicating that the aromatic amino acid residues moved towards more hydrophilic environments (Zhao et al., 2023), while the red-shift after the addition of RES suggested an increase in the hydrophobicity of the microenvironment of the aromatic amino acid residues (Tang, Li, Bi, & Gao, 2016). Visible absorption peaks at wavelengths of near 425, 370, and 325 nm were observed after complexion with RP, revealing the typical groups in CUR/QUE/RES, which also provided a dose dependent behavior with increased polyphenol concentration.

Molecular forces

In Fig. S4, variations in endogenous fluorescence intensity for the three complexes were depicted following the introduction of different denaturants. The addition of disruptive solvents dismantled forces between the protein and polyphenol, with changes in fluorescence intensity reflecting this disruption. As shown in the Fig. S4, all three complexes exhibited the most substantial increase in fluorescence intensity after the addition of SDS, while changes were comparatively smaller after the introduction of the other two reagents. This suggested that the primary driving force for the binding between RP and CUR/QUE/RES was hydrophobic interaction, with hydrogen bonding and intermolecular forces playing auxiliary roles. This aligned with similar findings in previous studies. For instance, the complexation of rice glutenin with resveratrol (Dai, Li, et al., 2019), as well as soy protein with resveratrol (Wan et al., 2014), was also primarily driven by hydrophobic forces. In the case of rice protein and curcumin (Xu et al., 2022), the interaction was driven by hydrogen bonding and hydrophobic attraction. Additionally, the change in fluorescence intensity of RP-QUE after the addition of urea is the most pronounced among the three complexes, which is also consistent with the results of molecular docking simulations in which RP-QUE has the highest number of hydrogen bonds.

Computational docking simulation

In order to gain deeper insights into the interactions between three polyphenols and RP, computational docking simulations were employed. CUR, QUE, and RES formed stable complexes with glutelin, exhibiting significant affinity as demonstrated by their binding energies (CUR: −6.83 kcal/mol, QUE: −6.96 kcal/mol, RES: −7.12 kcal/mol). The binding energy sizes followed the order RES > QUE > CUR. The results obtained may also be related to the molecular weight (RES: 228.24, QUE: 302.24, CUR: 368.38) and complexity of the small molecules themselves (RES: 248, QUE: 488, CUR: 507). Compared with RES, the small number of rotatable bonds in QUE may limit its behavior in the simulated environment. These compounds effectively complemented the protein sites and established stable complexes with the proteins, thereby exhibiting a strong association with RP. The three compounds located in the similar groove pocket of RP with different interacting amino acids (Fig. 2A).

Fig. 2E–M displayed the 2D schematic diagram of specific amino acid residues engaged in compound binding within the protein pockets. For CUR, two hydrogen bonds were formed with the residues of ARG 292 and GLU 373. Van der Waals Force with ALA 90, GLN 91, ARG 132, GLU 133, GLY 134, GLY 291, SER 293, ASN 289, ARG 326, THR 350, GLU 395 and hydrophobic interaction with ARG292, ARG 351 were formed between CUR and glutelin. QUE interacted with rice glutelin, forming van der Waals interactions with surrounding active amino acids including PHE 88, ARG 132, ASN 289, GLY 291, SER 293, THR 350, ARG 351, and hydrophobic interaction of ARG292 and ARG 326. In addition, QUE established hydrogen bonds with ALA 90, GLU 133, ARG 292, and GLU395. Notably, a higher number of hydrogen bonds were observed between the amino acids of rice glutelin and the phenolic hydroxyl groups of QUE compared to CUR and RES.

RES, characterized by two hydrophobic benzene rings, established robust hydrophobic interactions with key amino acids (ALA 90, GLU 133, ARG 326, GLU 395) located at the active site. Additionally, the benzene ring of RES formed hydrophobic interaction with residules of ALA 90, GLU 133, ARG 326, GLU 395, further enhancing the stabilization of small molecules within the protein cavity. Moreover, RES formed three strong hydrogen bonds with GLN 91, TYR 348, and GLU 373

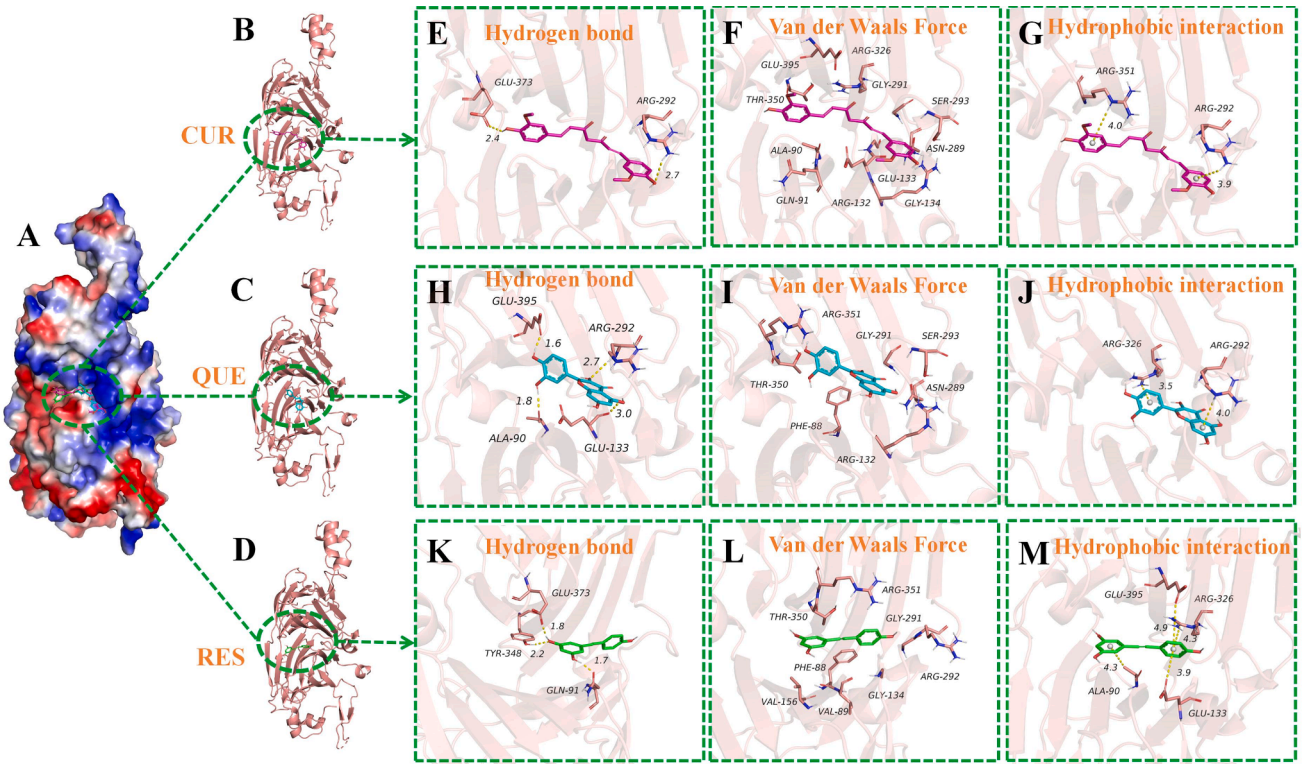

Fig. 2. (A): Modelling of RP binding to three polyphenols. (B-D): Models of RP binding to CUR, QUE, and RES, respectively. Amino acids involved in hydrogen bonding, van der Waals forces, and hydrophobic interactions in the binding of RP to CUR (E, F, G), QUE (H, I, J), and RES (K, L, M), respectively.

residues, crucially anchoring the small molecules within the protein cavity (Luo et al., 2021).

Circular dichroism spectra

To investigate the impact of binding on the conformation of RP, CD spectra of pure protein and its complexes with CUR/QUE/RES were obtained and analyzed (Fig. 3A). CD data revealed that the α-helix, β-sheet, β-turn, and random coil fractions in the free protein were 7.07 %, 35.57 %, 22.82 %, and 34.53 %, respectively, consistent with a previous study (Dai, Li, et al., 2019). After incorporation of CUR/QUE/RES, a reduction in the α-helical fraction and an increase in the β-sheet fraction were observed, suggesting that the polyphenols likely inserted themselves into the hydrophobic regions of RP molecules, disrupting the hydrogen bonding networks. This led to the unfolding of the protein and enhanced molecular flexibility (Xu et al., 2019). The decrease in α-helical structure is hypothesized to be advantageous for emulsification characteristics, as it enables rapid structural changes upon adsorption at the oil–water interface (Flores-Jiménez et al., 2019). No significant changes were observed in the β-turn and random coil fractions of RP with or without polyphenols ($p > 0.05$). Noteworthy, among the three compounds, QUE exhibited the most pronounced impact on the secondary structure of RP. This effect may be attributed to the fact that QUE disrupted the hydrogen bonds between protein molecules, which plays a key role in stabilizing the secondary structure of proteins. This is consistent with the results of fluorescence quenching (Section 'Fluorescence quenching mechanism').

FTIR spectra

RP, pure polyphenols, and their complexes were subjected to FTIR spectroscopy for structural analysis (Fig. 3B). RP exhibited an Amide I band (1700–1600 cm^{-1}) at 1659 cm^{-1}, an Amide II band (1550–1450 cm^{-1}) at 1547 cm^{-1}, and an Amide III at 1240 cm^{-1} (1450–1200 cm^{-1}), respectively. The individual spectra of CUR/QUE/RES exhibited characteristic peaks, consistent with our previous findings (Zhang, Wang, et al., 2022). However, in the complexes, most of these characteristic peaks became less prominent, indicating the binding of polyphenols to the protein and the resulting restriction in molecular vibration and stretching (Zhan, Dai, Zhang, & Gao, 2020).

Of particular interest is the region between 1700 and 1600 cm^{-1}, which is commonly utilized to assess changes in protein secondary structure. A slight red-shift was observed in the Amide I band for pure protein from 1659 to 1666, 1666, and 1665 cm^{-1} for RP-CUR, RP-QUE, and RP-RES, respectively. This observation was consistent with the results of CD spectroscopy analysis, which also indicated alterations in the protein's secondary structure.

Particle size and zeta potential of rice protein-polyphenols complexes

Fig. 4A–B displays the particle size and zeta potential of RP and its complexes with three polyphenolic substances. Pure protein exhibited a particle size of approximately 140 nm with a PDI value of 0.3. Addition of CUR did not induce significant changes in particle size and distribution ($p > 0.05$). Conversely, the hydrodynamic particle size significantly increased to 145 and 146 nm after combination with QUE and RES ($p < 0.05$), respectively, while maintaining a nearly unchanged size distribution. These results indicate that the complex samples represent uniformly distributed colloidal solutions with small particle dimensions, which are advantageous for potential applications as nanoscale delivery systems.

RP displayed a surface charge of approximately −35 mV, and the addition of CUR/QUE/RES did not cause any significant changes ($p > 0.05$). This observation can be attributed to the incorporation of CUR/QUE/RES into the hydrophobic pocket of RP, which did not alter the surface charge. Furthermore, the hydroxyl groups on the CUR/QUE/RES molecules were predominantly non-ionized or only slightly ionized, resulting in negligible surface charge at pH 7 (Peng et al., 2019).

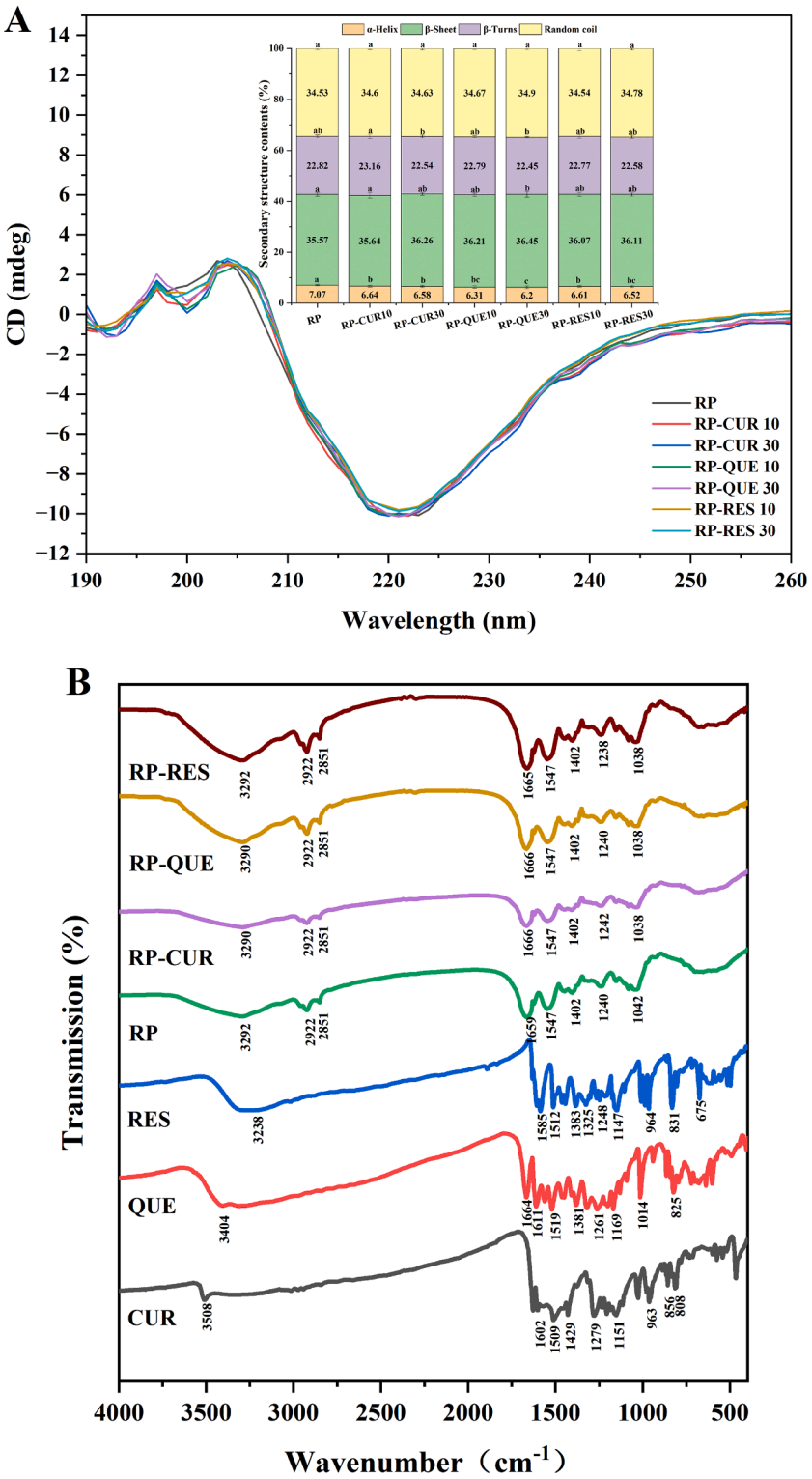

Fig. 3. CD spectra and secondary structure fractions of RP with or without CUR, QUE, RES (A). FTIR spectra of RP, CUR, QUE, RES and binary complexes of RP and polyphenols (B). Note: Different letters (Fig. 2 A) indicated the significantly different values between samples ($p < 0.05$).

Antioxidant properties of rice protein-polyphenols complexes

Antioxidant properties of both pure protein and non-covalent complexes were investigated using DPPH and ABTS radical scavenging assays (Fig. 4C–D). RP exhibited antiradical activities, primarily attributed to its content of sulfur-containing amino acids (Amagliani, O'Regan, Kelly, & O'Mahony, 2017). Compared to the protein control, all the complexes demonstrated enhanced inhibition of free radical chain reactions, which can be attributed to the incorporation of hydroxyl groups from the polyphenols into the system. Similar synergistic antioxidant effects have been observed between soy protein and anthocyanin (Ju et al., 2020). It has also been shown previously that binding between protein and polyphenol can also produce a better synergistic effect, with the resulting binary complexes exhibiting significantly higher

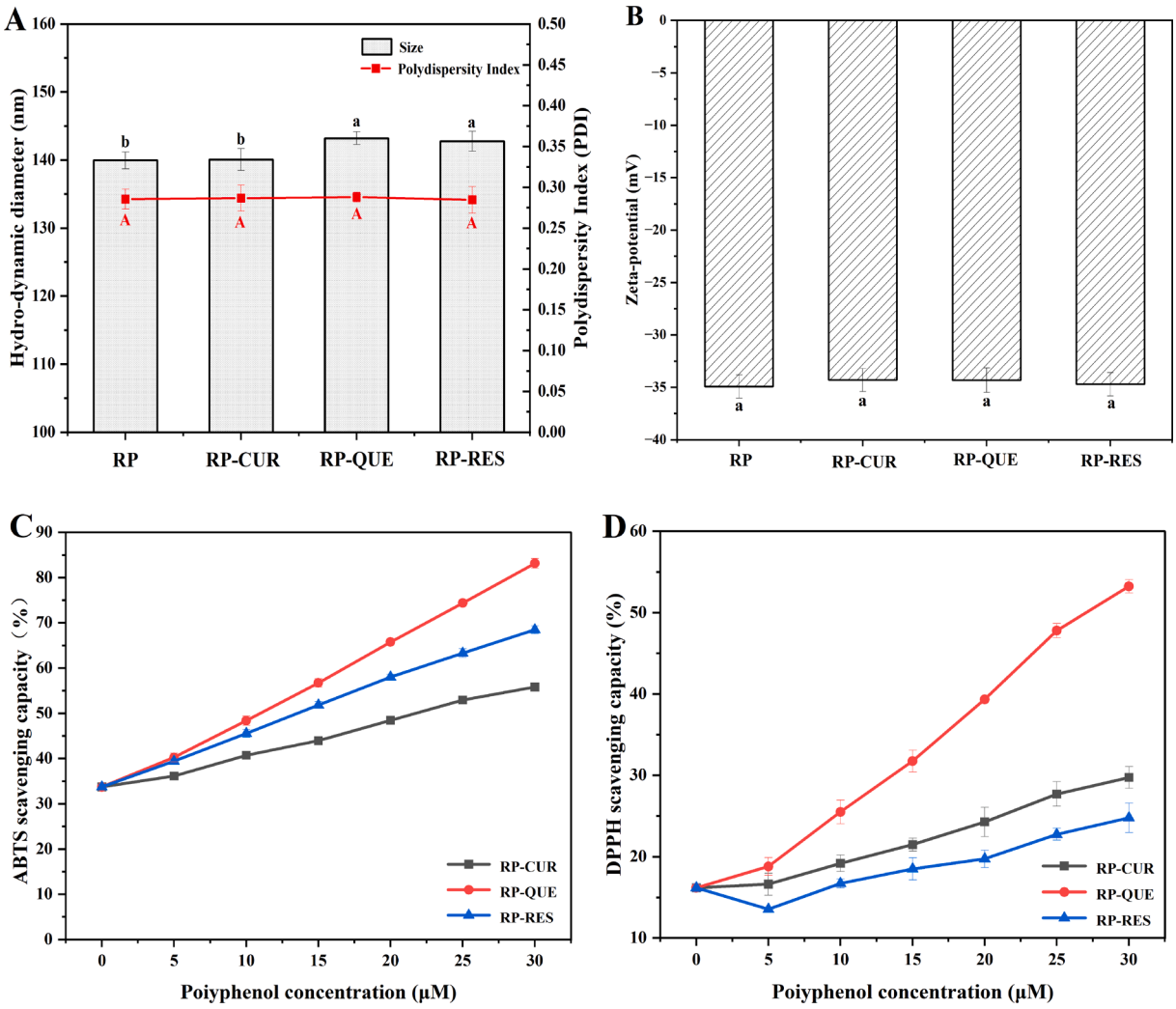

Fig. 4. Particle size and polydispersity index (A), zeta potential (B) of the RP, RP-CUR, RP-QUE, and RP-RES. ABTS scavenging capacity (C) and DPPH scavenging capacity (D) of RP-CUR, RP-QUE, and RP-RES. Note: The different letters represent significant difference between samples ($p < 0.05$).

antioxidant activity than free polyphenol, which may be related to the fact that binding of hydrophobic polyphenol to protein improves solubility and thus increases contact with free radicals (Li et al., 2022). Furthermore, the antioxidant capacity of the polyphenol complexes exhibited a dose-dependent relationship as their concentrations increased. Among the three polyphenols, QUE exhibited the most significant impact on improving the antioxidant capacity of RP. This observation aligns with the findings from the ABTS test. The superior free radical scavenging capacity of QUE can be attributed to the abundance of hydroxyl groups within its molecular structure as shown in Fig. 1. Based on the results of the antioxidant properties of the complexes, we deduced that emulsions prepared with protein–polyphenol complexes as emulsifiers may have better anti-lipid oxidation performance compared to emulsions prepared solely using RP as the emulsifying agent (Cao et al., 2023).

Characterization of emulsion

Particle size of emulsions stabilized by rice protein-polyphenols complexes

Fig. 5B presents the particle size distribution of the emulsions, which measured 470 nm with a PDI of approximately 0.4 for the protein-stabilized emulsion. These findings align with a previous study where emulsions stabilized by rice glutelin (1 % and 2 % protein concentrations) exhibited surface-weighted mean droplet diameter (D[3,2]) values ranging from 0.73 to 1.94 μm (Agboola, Ng, & Mills, 2005). The complexes-stabilized emulsions, compared to the control, exhibited significantly smaller particle size ($p < 0.05$). Moreover, emulsions stabilized by CUR/RES complexes displayed notably smaller particle size than RP-QUE emulsions (378–395 nm, $p < 0.05$). This reduction could be attributed to the formation of a dense interfacial structure through peptide chain cross-linking between proteins and polyphenols. Additionally, the combination with polyphenols may enhance the interfacial activity of protein, accelerate interface adsorption, and subsequently reduce the particle size of the emulsion (Liu et al., 2022).

Surface charge of emulsions stabilized by rice protein-polyphenols complexes

Droplet surface charge plays a pivotal role in elucidating the colloidal stability of emulsions and the intricate electrostatic interactions within food systems (Liu et al., 2022). As depicted in Fig. 5C, the emulsion stabilized by RP displayed a zeta potential of −35.6 mV, indicative of a formidable electrostatic repulsion force and a substantial interdroplet separation distance. This pronounced surface charge confers exceptional stability upon the emulsion (Liu et al., 2022). Intriguingly, all complex emulsions exhibited significantly elevated absolute zeta potential values ($p < 0.05$), underscoring their augmented electronegativity. The intensified surface charge of the complex emulsions engenders a formidable energy barrier between the emulsion droplets, thus endowing them with heightened electrostatic repulsion capabilities and an inherent resistance against undesirable phenomena such as coalescence and flocculation (Li et al., 2020). The augmentation in

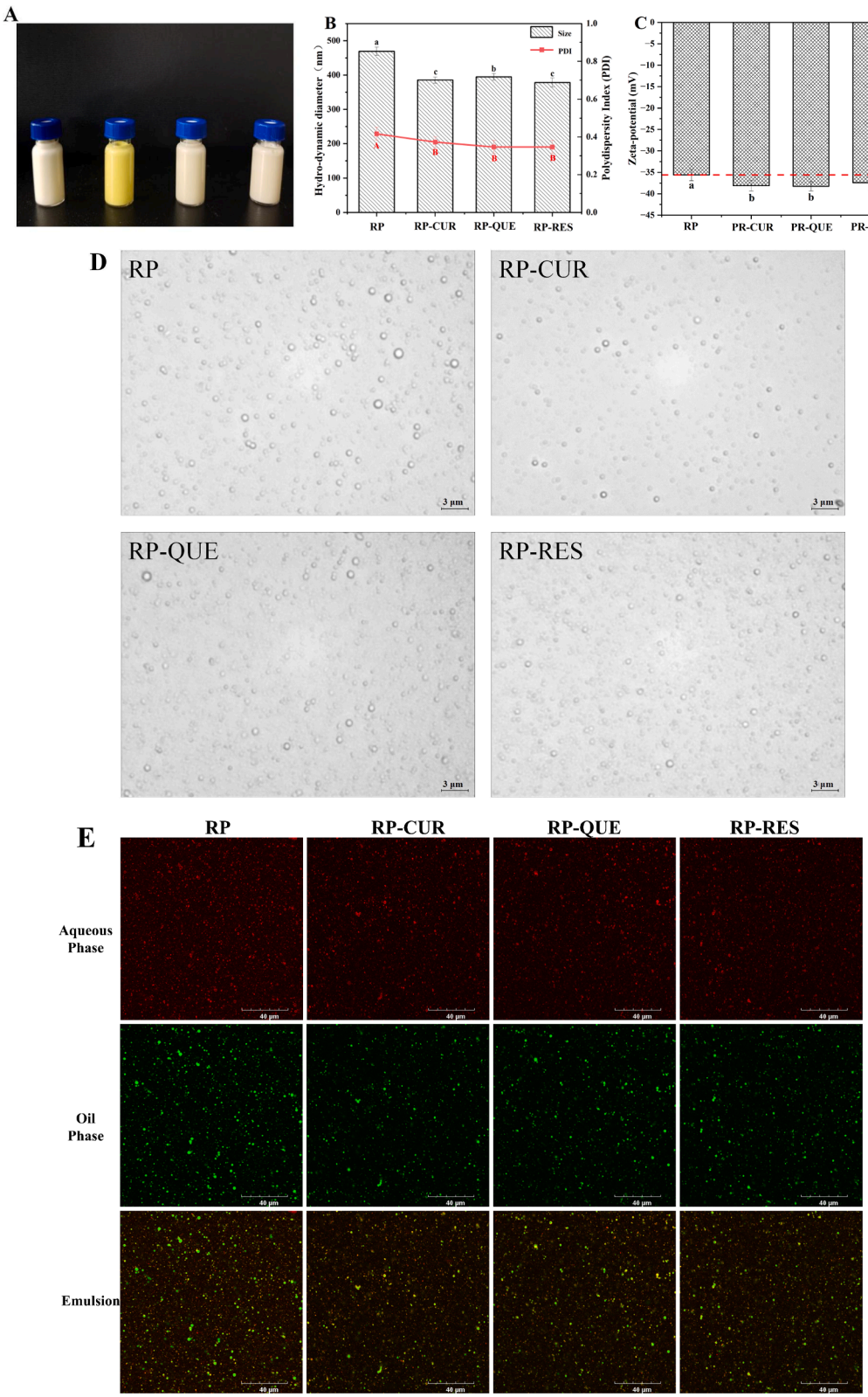

Fig. 5. Appearance images (A) of the emulsions prepared by RP, RP-CUR, RP-QUE, and RP-RES. Particle size and polydispersity index (B), zeta potential (C), and microscope images (D) of the emulsions. Laser confocal microscopy images (E) of emulsions, the scale bar was 40 μm in length. Note: The different letters represent significant difference between samples ($p < 0.05$).

surface charge can be attributed to the modulating influence of RES/CUR/QUE on the secondary structure of RP, resulting in the exposure of more negatively charged amino acid residues or a reduction in positively charged moieties.

Microstructure of emulsions stabilized by rice protein-polyphenols complexes

Microstructural analysis was performed on emulsions stabilized by RP and its complexes, as illustrated in Fig. 5D. The microstructural images provided visual confirmation of the enhanced physical stability achieved through the incorporation of CUR/QUE/RES into the emulsions. Emulsions stabilized solely by RP exhibited larger particle size with relatively inhomogeneous distribution. In contrast, the remaining three emulsions demonstrated a homogeneous distribution with reduced particle size.

The distribution and microstructure of emulsion samples (RP, RP-CUR, RP-QUE, and RP-RES) were studied using laser confocal microscopy. As shown in Fig. 5E, the presence of a red ring surrounding the green spheres in the emulsion phase indicates the formation of an oil-in-water emulsion (Zhang, Zhang, et al., 2022). The reduction in the number of larger green spheres in the oil and emulsion phases of the three emulsion samples supplemented with polyphenols suggests that the droplet size of the samples increased uniformity. Fig. S5 shows the images of the protein phase under an oil immersion lens, clearly revealing that the RP emulsion samples have larger sizes in the red area, whereas the protein in the other samples are smaller and more uniform in size.

Lipid oxidation of emulsions stabilized by rice protein-polyphenols complexes

In emulsions, lipid oxidation commonly occurs at the oil–water interface, resulting from interactions between hydrophilic pro-oxidants (such as transition metal ions and photosensitizers) from the aqueous phase and hydrophobic lipid substrates from the oil phase (Liang et al., 2017; Walker, Gumus, Decker, & McClements, 2017). Lipid oxidation leads to sensory quality and nutritive value deterioration, as well as the formation of potentially harmful end products (Walker et al., 2017), and addition of antioxidants is a common strategy to retard or prevent lipid peroxidation. The effectiveness of an antioxidant is largely determined by its radical scavenging or chelating ability and its interaction with other reactants (Kim, Kim, & Lee, 2018).

The evolution of primary and secondary oxidation products was measured in emulsions stored for up to 10 days (Fig. 6). The initial emulsions already exhibited PV and TBARS values, which may be attributed to oxidation products present in the raw materials. As the storage time progressed, lipid oxidation became more pronounced, leading to rapid growth in both PV and TBARS values for all emulsion samples. However, the slope of the oxidation curve varied among the emulsions, indicating differences in the rate of lipid oxidation. Specifically, emulsions stabilized with RP alone exhibited the highest lipid oxidation rate, while addition of the three compounds resulted in a retardation of oxidation, with QUE showing the highest inhibition effectiveness, followed by CUR and RES. This trend aligns with the antioxidant properties results (Fig. 4A–B). The data indicated that emulsions stabilized with RP complexes were more stable compared to those stabilized with RP alone, as the incorporation of QUE/CUR/RES introduced more hydroxyl groups, thereby increasing the hydrogen supply capacity of the protein and protecting the emulsion from oxidation.

The relatively lower rate of lipid oxidation observed in the three complexes coated emulsions can be attributed to their inherent antioxidant activity, which can break free radical chain reactions and reduce the content of low-valence vivacious metal elements, thereby directly inhibiting lipid oxidation (Zhang et al., 2021). Additionally, smaller particle sizes have been shown to enhance oxidation stability (Duan et al., 2016), and the small particle size of the complexes-stabilized emulsion may also contribute to its higher stability. Furthermore, previous studies have shown a correlation between the impact of polyphenols on lipid oxidation in emulsions and their oil–water partition coefficient (Log P) value (Mansouri, Farhoosh, & Rezaei, 2020). The Log P values of CUR, QUE, and RES were 3.2, 1.5, and 3.1, respectively. Therefore, the superior ability of QUE to inhibit lipid oxidation may be attributed to its minimum Log P value and its unique chemical structure. This suggests that some QUE may be distributed in the water phase, effectively inhibiting lipid oxidation.

Conclusions

This study aimed to explore the non-covalent interactions between CUR/ QUE/RES and RP and evaluate the potential application in emulsions. The three polyphenols bound to RP with relatively strong affinity, with binding affinities ranking in the order of QUE > CUR > RES. Polyphenols induced alterations in the secondary structure of RP, with QUE causing the greatest changes. The formed complexes can be used as novel emulsifiers to fabricate emulsions with small particle size, higher surface charge, and higher oxidative stability. These findings provide insightful contributions to the development of functional ingredients that merge proteins and polyphenols for emulsion-based delivery systems.

CRediT authorship contribution statement

Xin Huang: Writing – original draft, Methodology, Investigation, Data curation. **Boxue Xia:** Investigation. **Yaxuan Liu:** Methodology.

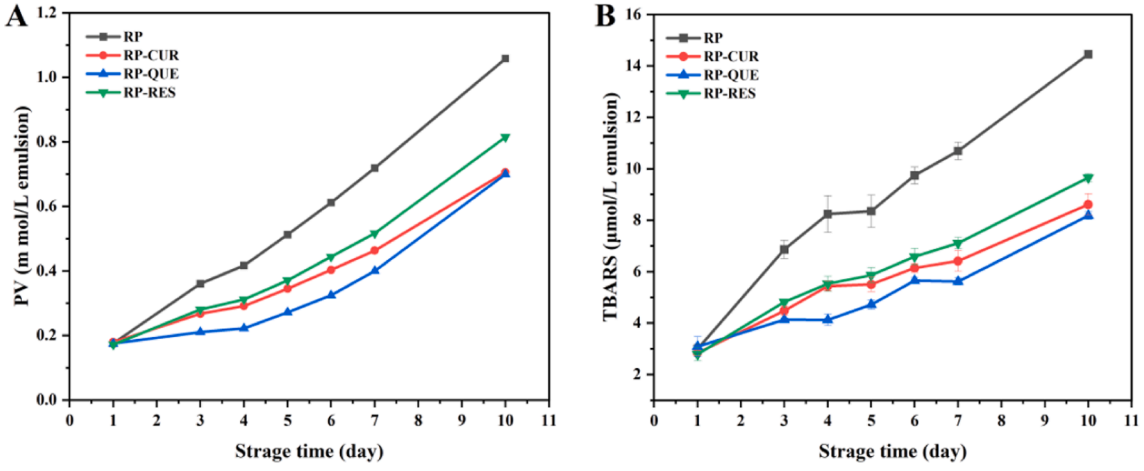

Fig. 6. PV values (A) and TBARS values (B) of the emulsions prepared by RP, RP-CUR, RP-QUE, and RP-RES during 10-days storage.

Cuina Wang: Project administration, Funding acquisition.

Declaration of competing interest

The authors declare that they have no known competing financial interests or personal relationships that could have appeared to influence the work reported in this paper.

Data availability

Data will be made available on request.

Acknowledgments

This study was financially supported by Key Scientific & Technological Projects of Jilin Provincial Science and Technology Department (Project no. 20210204036YY).

Appendix A. Supplementary material

Supplementary data to this article can be found online at https://doi.org/10.1016/j.fochx.2024.101459.

References

Agboola, S., Ng, D., & Mills, D. (2005). Characterisation and functional properties of Australian rice protein isolates. *Journal of Cereal Science, 41*(3), 283–290. https://doi.org/10.1016/j.jcs.2004.10.007

Amagliani, L., O'Regan, J., Kelly, A. L., & O'Mahony, J. A. (2017). The composition, extraction, functionality and applications of rice proteins: A review. *Trends in Food Science & Technology, 64*, 1–12. https://doi.org/10.1016/j.tifs.2017.01.008

Baek, M., & Mun, S. (2022). Improvement of the water solubility and emulsifying capacity of rice proteins through the addition of isolated soy protein. *International Journal of Food Science & Technology, 57*(7), 4411–4421. https://doi.org/10.1111/ijfs.15772

Cao, Y., Zang, Z., Zhang, L., Han, G., Yu, Q., & Han, L. (2023). Hydroxypropyl methyl cellulose/soybean protein isolate nanoparticles incorporated broccoli leaf polyphenol to effectively improve the stability of Pickering emulsions. *International Journal of Biological Macromolecules, 250*, Article 126269. https://doi.org/10.1016/j.ijbiomac.2023.126269

Cen, S., Li, Z., Guo, Z., Li, H., Shi, J., Huang, X., Zou, X., & Holmes, M. (2022). 4D printing of a citrus pectin/β-CD Pickering emulsion: A study on temperature induced color transformation. *Additive Manufacturing, 56*, Article 102925. https://doi.org/10.1016/j.addma.2022.102925

Chen, W., Ju, X., Aluko, R. E., Zou, Y., Wang, Z., Liu, M., & He, R. (2020). Rice bran protein-based nanoemulsion carrier for improving stability and bioavailability of quercetin. *Food Hydrocolloids, 108*, Article 106042. https://doi.org/10.1016/j.foodhyd.2020.106042

Chen, Y., Yao, M., Peng, S., Fang, Y., Wan, L., Shang, W., Xiang, D., & Zhang, W. (2023). Development of protein-polyphenol particles to stabilize high internal phase Pickering emulsions by polyphenols' structure. *Food Chemistry, 428*, Article 136773. https://doi.org/10.1016/j.foodchem.2023.136773

Chen, X., Zhao, H., Wang, H., Xu, P., Chen, M., Xu, Z., Wen, L., Cui, B., Yu, B., Zhao, H., Jiao, Y., & Cheng, Y. (2022). Preparation of high-solubility rice protein using an ultrasound-assisted glycation reaction. *Food Research International, 161*, Article 111737. https://doi.org/10.1016/j.foodres.2022.111737

Dai, T., Chen, J., McClements, D. J., Hu, P., Ye, X., Liu, C., & Li, T. (2019). Protein-polyphenol interactions enhance the antioxidant capacity of phenolics: Analysis of rice glutelin-procyanidin dimer interactions. *Food & Function, 10*(2), 765–774. https://doi.org/10.1039/c8fo02246a

Dai, T., Li, R., Liu, C., Liu, W., Li, T., Chen, J., Kharat, M., & McClements, D. J. (2019). Effect of rice glutelin-resveratrol interactions on the formation and stability of emulsions: A multiphotonic spectroscopy and molecular docking study. *Food Hydrocolloids, 97*, Article 105234. https://doi.org/10.1016/j.foodhyd.2019.105234

Dai, T., Yan, X., Li, Q., Li, T., Liu, C., McClements, D. J., & Chen, J. (2017). Characterization of binding interaction between rice glutelin and gallic acid: Multi-spectroscopic analyses and computational docking simulation. *Food Research International, 102*, 274–281. https://doi.org/10.1016/j.foodres.2017.09.020

Dai, H., Zhan, F., Chen, Y., Shen, Q., Geng, F., Zhang, Z., & Li, B. (2022). Improvement of the solubility and emulsification of rice protein isolate by the pH shift treatment. *International Journal of Food Science & Technology, 58*(1), 355–366. https://doi.org/10.1111/ijfs.15834

Duan, X., Li, M., Ma, H., Xu, X., Jin, Z., & Liu, X. (2016). Physicochemical properties and antioxidant potential of phosvitin–resveratrol complexes in emulsion system. *Food Chemistry, 206*, 102–109. https://doi.org/10.1016/j.foodchem.2016.03.055

Flores-Jiménez, N. T., Ulloa, J. A., Silvas, J. E. U., Ramírez, J. C. R., Ulloa, P. R., Rosales, P. U. B., Carrillo, Y. S., & Leyva, R. G. (2019). Effect of high-intensity ultrasound on the compositional, physicochemical, biochemical, functional and structural properties of canola (Brassica napus L.) protein isolate. *Food Research International, 121*, 947–956. https://doi.org/10.1016/j.foodres.2019.01.025

Ghanghas, N., Mukilan, M. T., Sharma, S., & Prabhakar, P. K. (2022). Classification, composition, extraction, functional modification and application of rice (Oryza sativa) seed protein: A comprehensive review. *Food Reviews International, 38*(4), 354–383. https://doi.org/10.1080/87559129.2020.1733596

Guo, Y., Wang, M., Xing, K., Pan, M., & Wang, L. (2023). Covalent binding of ultrasound-treated japonica rice bran protein to catechin: Structural and functional properties of the complex. *Ultrasonics Sonochemistry, 93*, Article 106292. https://doi.org/10.1016/j.ultsonch.2023.106292

Han, S., Cui, F., McClements, D. J., Xu, X., Ma, C., Wang, Y., Liu, X., & Liu, F. (2022). Structural characterization and evaluation of interfacial properties of pea protein isolate–EGCG molecular complexes. *Foods, 11*(18), Article 2895. https://doi.org/10.3390/foods11182895

Huang, X., Sun, L., Liu, L., Wang, G., Luo, P., Tang, D., & Huang, Q. (2022). Study on the mechanism of mulberry polyphenols inhibiting oxidation of beef myofibrillar protein. *Food Chemistry, 372*, Article 131241. https://doi.org/10.1016/j.foodchem.2021.131241

Ismail, B. P., Senaratne-Lenagala, L., Stube, A., & Brackenridge, A. (2020). Protein demand: Review of plant and animal proteins used in alternative protein product development and production. *Animal Frontiers, 10*(4), 53–63. https://doi.org/10.1093/af/vfaa040

Jiang, Z., Gan, J., Wang, L., & Lv, C. (2023). Binding of curcumin to barley protein Z improves its solubility, stability and bioavailability. *Food Chemistry, 399*, Article 133952. https://doi.org/10.1016/j.foodchem.2022.133952

Ju, M., Zhu, G., Huang, G., Shen, X., Zhang, Y., Jiang, L., & Sui, X. (2020). A novel pickering emulsion produced using soy protein-anthocyanin complex nanoparticles. *Food Hydrocolloids, 99*, Article 105329. https://doi.org/10.1016/j.foodhyd.2019.105329

Kim, J., Kim, M.-J., & Lee, J. (2018). The critical micelle concentration of lecithin in bulk oils and medium chain triacylglycerol is influenced by moisture content and total polar materials. *Food Chemistry, 261*, 194–200. https://doi.org/10.1016/j.foodchem.2018.04.048

Li, C., Dai, T., Chen, J., Li, X., Li, T., Liu, C., & McClements, D. J. (2021). Protein-polyphenol functional ingredients: The foaming properties of lactoferrin are enhanced by forming complexes with procyanidin. *Food Chemistry, 339*, Article 128145. https://doi.org/10.1016/j.foodchem.2020.128145

Li, T., Wang, L., Zhang, X., Yu, P., & Chen, Z. (2021). Complexation of rice glutelin fibrils with cyanidin-3-O-glucoside at acidic condition: Thermal stability, binding mechanism and structural characterization. *Food Chemistry, 363*, Article 130367. https://doi.org/10.1016/j.foodchem.2021.130367

Li, Z. Y., Wang, J. Y., Zheng, B. D., & Guo, Z. B. (2019). Effects of high pressure processing on gelation properties and molecular forces of myosin containing deacetylated konjac glucomannan. *Food Chemistry, 291*, 117–125. https://doi.org/10.1016/j.foodchem.2019.03.146

Li, W., Yu, Y., Dai, Z., Peng, J., Wu, J., & Wang, Z. (2022). Encapsulation of curcumin in a ternary nanocomplex prepared with carboxymethyl short linear glucan–sodium–caseinate–pectin via electrostatic interactions. *Journal of Food Science*. https://doi.org/10.1111/1750-3841.16026

Li, D., Zhao, Y., Wang, X., Tang, H., Wu, N., Wu, F., Yu, D., & Elfalleh, W. (2020). Effects of (+)-catechin on a rice bran protein oil-in-water emulsion: Droplet size, zeta-potential, emulsifying properties, and rheological behavior. *Food Hydrocolloids, 98*, Article 105306. https://doi.org/10.1016/j.foodhyd.2019.105306

Liang, L., Chen, F., Wang, X., Jin, Q., Decker, E. A., & McClements, D. J. (2017). Physical and oxidative stability of flaxseed oil-in-water emulsions fabricated from sunflower lecithins: Impact of blending lecithins with different phospholipid profiles. *Journal of Agricultural and Food Chemistry, 65*(23), 4755–4765. https://doi.org/10.1021/acs.jafc.7b01469

Liu, J. X., Gao, T. T., Li, F. L., & Xie, T. (2022). The addition of oxidized tea polyphenols enhances the physical and oxidative stability of rice bran protein hydrolysate-stabilized oil-in-water emulsions. *Food Science and Technology Research, 28*(3), 225–233. https://doi.org/10.3136/fstr.FSTR-D-21-00248

Liu, R., Liu, Q., Xiong, S., Fu, Y., & Chen, L. (2017). Effects of high intensity unltrasound on structural and physicochemical properties of myosin from silver carp. *Ultrasonics Sonochemistry, 37*(1), 150–157. https://doi.org/10.1016/j.ultsonch.2016.12.039

Liu, C., Yang, X., Wu, W., Long, Z., Xiao, H., Luo, F., Shen, Y., & Lin, Q. (2018). Elaboration of curcumin-loaded rice bran albumin nanoparticles formulation with increased in vitro bioactivity and in vivo bioavailability. *Food Hydrocolloids, 77*, 834–842. https://doi.org/10.1016/j.foodhyd.2017.11.027

Lu, Y., Zhao, R., Wang, C., Zhang, X., & Wang, C. (2022). Deciphering the non-covalent binding patterns of three whey proteins with rosmarinic acid by multi-spectroscopic, molecular docking and molecular dynamics simulation approaches. *Food Hydrocolloids, 132*, Article 107895. https://doi.org/10.1016/j.foodhyd.2022.107895

Luo, W., Huang, H., Zhang, Y., Wang, F., Yu, J., Liu, Y., & Li, X. (2021). Complex coacervation behavior and the mechanism between rice glutelin and gum arabic at pH 3.0 studied by turbidity, light scattering, fluorescence spectra and molecular docking. *LWT - Food Science & Technology, 150*, Article 112084. https://doi.org/10.1016/j.lwt.2021.112084

Mansouri, H., Farhoosh, R., & Rezaei, M. (2020). Interfacial performance of gallic acid and methyl gallate accompanied by lecithin in inhibiting bulk phase oil peroxidation. *Food Chemistry, 328*, Article 127128. https://doi.org/10.1016/j.foodchem.2020.127128

Pan, X., Fan, F., Ding, J., Li, P., Sun, X., Zhong, L., & Fang, Y. (2022). Altering functional properties of rice protein hydrolysates by covalent conjugation with chlorogenic

acid. *Food Chemistry: X, 14*, Article 100352. https://doi.org/10.1016/j.fochx.2022.100352

Parolia, S., Maley, J., Sammynaiken, R., Green, R., Nickerson, M., & Ghosh, S. (2022). Structure – Functionality of lentil protein-polyphenol conjugates. *Food Chemistry, 367*, Article 130603. https://doi.org/10.1016/j.foodchem.2021.130603

Peng, H., Gan, Z., Xiong, H., Luo, M., Yu, N., Wen, T., Wang, R., & Li, Y. (2017). Self-assembly of protein nanoparticles from rice bran waste and their use as delivery system for curcumin. *ACS Sustainable Chemistry and Engineering, 5*(8), 6605–6614. https://doi.org/10.1021/acssuschemeng.7b00851

Peng, S., Zou, L., Zhou, W., Liu, W., Liu, C., & McClements, D. J. (2019). Encapsulation of lipophilic polyphenols into nanoliposomes using pH-driven method: Advantages and disadvantages. *Journal of Agricultural and Food Chemistry, 67*(26), 7506–7511. https://doi.org/10.1021/acs.jafc.9b01602

Roy, T., Singh, A., Sari, T. P., & Homroy, S. (2023). Rice protein: Emerging insights of extraction, structural characteristics, functionality, and application in the food industry. *Journal of Food Composition and Analysis, 123*, Article 105581. https://doi.org/10.1016/j.jfca.2023.105581

Su, C., He, Z., & Li, H. (2022). Covalent interactions between rabbit myofibrillar proteins and quercetin: A promising approach to enhance protein antioxidant capacity and thermal stability. *LWT - Food Science and Technology, 171*, Article 114132. https://doi.org/10.1016/j.lwt.2022.114132

Sun, L. H., Lv, S. W., Chen, C. H., & Wang, C. (2019). Preparation and characterization of rice bran protein-stabilized emulsion by using ultrasound homogenization. *Cereal Chemistry, 96*(3), 478–486. https://doi.org/10.1002/cche.10147

Tang, L., Li, S., Bi, H. N., & Gao, X. (2016). Interaction of cyanidin-3-O-glucoside with three proteins. *Food Chemistry, 196*, 550–559. https://doi.org/10.1016/j.foodchem.2015.09.089

Tu, Y., Zhang, X., & Wang, L. (2023). Effect of salt treatment on the stabilization of Pickering emulsions prepared with rice bran protein. *Food Research International, 166*, Article 112537. https://doi.org/10.1016/j.foodres.2023.112537

Walker, R. M., Gumus, C. E., Decker, E. A., & McClements, D. J. (2017). Improvements in the formation and stability of fish oil-in-water nanoemulsions using carrier oils: MCT, thyme oil, & lemon oil. *Journal of Food Engineering, 211*, 60–68. https://doi.org/10.1016/j.jfoodeng.2017.05.004

Wan, Z., Wang, J., Wang, L., Yuan, Y., & Yang, X. (2014). Complexation of resveratrol with soy protein and its improvement on oxidative stability of corn oil/water emulsions. *Food Chemistry, 161*, 324–331. https://doi.org/10.1016/j.foodchem.2014.04.028

Wang, C., Cui, B., Sun, Y., Wang, C., & Guo, M. (2022). Preparation, stability, antioxidative property and in vitro release of cannabidiol (CBD) in zein-whey protein composite nanoparticles. *LWT - Food Science & Technology, 162*, Article 113466. https://doi.org/10.1016/j.lwt.2022.113466

Wang, T., Xu, P. C., Chen, Z. X., Zhou, X., & Wang, R. (2018). Alteration of the structure of rice proteins by their interaction with soy protein isolates to design novel protein composites. *Food & Function, 9*(8), 4282–4291. https://doi.org/10.1039/c8fo00661j

Wang, C., Zhang, X., Zhao, R., Freeman, K., McHenry, M. A., Wang, C., & Guo, M. (2022). Impact of carrier oil on interfacial properties, CBD partition and stability of emulsions formulated by whey protein or whey protein-maltodextrin conjugate. *LWT - Food Science & Technology, 168*, Article 113933. https://doi.org/10.1016/j.lwt.2022.113933

Xu, Y., Dai, T., Li, T., Huang, K., Li, Y., Liu, C., & Chen, J. (2019). Investigation on the binding interaction between rice glutelin and epigallocatechin-3-gallate using spectroscopic and molecular docking simulation. *Spectrochimica Acta Part A: Molecular and Biomolecular Spectroscopy, 217*, 215–222. https://doi.org/10.1016/j.saa.2019.03.091

Xu, P., Qian, Y., Wang, R., Chen, Z., & Wang, T. (2022). Entrapping curcumin in the hydrophobic reservoir of rice proteins toward stable antioxidant nanoparticles. *Food Chemistry, 387*, Article 132906. https://doi.org/10.1016/j.foodchem.2022.132906

Ye, J., Fan, F., Xu, X., & Liang, Y. (2013). Interactions of black and green tea polyphenols with whole milk. *Food Research International, 53*(1), 449–455. https://doi.org/10.1016/j.foodres.2013.05.033

Zhan, X., Dai, L., Zhang, L., & Gao, Y. (2020). Entrapment of curcumin in whey protein isolate and zein composite nanoparticles using pH-driven method. *Food Hydrocolloids, 106*, Article 105839. https://doi.org/10.1016/j.foodhyd.2020.105839

Zhang, M., Fan, L., Liu, Y., Huang, S., & Li, J. (2022). Effects of proteins on emulsion stability: The role of proteins at the oil–water interface. *Food Chemistry, 397*, Article 133726. https://doi.org/10.1016/j.foodchem.2022.133726

Zhang, X., Wang, C., Qi, Z., Zhao, R., Wang, C., & Zhang, T. (2022). Pea protein based nanocarriers for lipophilic polyphenols: Spectroscopic analysis, characterization, chemical stability, antioxidant and molecular docking. *Food Research International, 160*, Article 111713. https://doi.org/10.1016/j.foodres.2022.111713

Zhang, Y., Zhang, Y., Chen, N., Xin, N., Li, Q., Ye, H., Zhao, C., & Zhang, T. (2022). Glycated modification of the protein from Rana chensinensis eggs by Millard reaction and its stability analysis in curcumin encapsulated emulsion system. *Food Chemistry, 382*, Article 132299. https://doi.org/10.1016/j.foodchem.2022.132299

Zhang, Y., Zhao, M., Ning, Z., Yu, S., Tang, N., & Zhou, F. (2018). Development of a sono-assembled, bifunctional soy peptide nanoparticle for cellular delivery of hydrophobic active cargoes. *Journal of Agricultural and Food Chemistry, 66*(16), 4208–4218. https://doi.org/10.1021/acs.jafc.7b05889

Zhang, X., Zuo, Z., Yu, P., Li, T., Guang, M., Chen, Z., & Wang, L. (2021). Rice peptide nanoparticle as a bifunctional food-grade Pickering stabilizer prepared by ultrasonication: Structural characteristics, antioxidant activity, and emulsifying properties. *Food Chemistry, 343*, Article 128545. https://doi.org/10.1016/j.foodchem.2020.128545

Zhao, R., Lu, Y. C., Wang, C., Zhang, X. G., Khan, A., & Wang, C. A. (2023). Understanding molecular interaction between thermally modified β-lactoglobulin and curcumin by multi-spectroscopic techniques and molecular dynamics simulation. *Colloids and Surfaces B-Biointerfaces, 227*, Article 113334. https://doi.org/10.1016/j.colsurfb.2023.113334

Zhao, M., Xiong, W., Chen, B., Zhu, J., & Wang, L. (2020). Enhancing the solubility and foam ability of rice glutelin by heat treatment at pH12: Insight into protein structure. *Food Hydrocolloids, 103*, Article 105626. https://doi.org/10.1016/j.foodhyd.2019.105626

Zhong, M., Sun, Y., Song, H., Wang, S., Qi, B., Li, X., & Li, Y. (2023). Ethanol as a switch to induce soybean lipophilic protein self-assembly and resveratrol delivery. *Food Chemistry: X, 18*, Article 100698. https://doi.org/10.1016/j.fochx.2023.100698

Zhou, H., Zheng, B., & McClements, D. J. (2021). Encapsulation of lipophilic polyphenols in plant-based nanoemulsions: Impact of carrier oil on lipid digestion and curcumin, resveratrol and quercetin bioaccessibility. *Food & Function, 12*(8), 3420–3432. https://doi.org/10.1039/d1fo00275a